


## Effect of efavirenz-based ART on the pharmacokinetics of rifampicin and its primary metabolite in patients coinfecting with TB and HIV

Jesper Sundell <sup>1\*</sup>, Emile Bienvenu<sup>2</sup>, Angela Äbelö<sup>1</sup> and Michael Ashton<sup>1</sup>

<sup>1</sup>Unit for Pharmacokinetics and Drug Metabolism, Department of Pharmacology, Sahlgrenska Academy at University of Gothenburg, Gothenburg, Sweden; <sup>2</sup>Department of Pharmacy, School of Medicine and Pharmacy, University of Rwanda, Rwanda

\*Corresponding author. E-mail: jesper.sundell@gu.se

Received 22 December 2020; accepted 24 June 2021

**Objectives:** To evaluate the effects of concomitant efavirenz-based ART and genetic polymorphism on the variability in rifampicin and 25-desacetyl-rifampicin pharmacokinetics.

**Patients and methods:** Plasma concentrations of rifampicin and 25-desacetyl-rifampicin from 63 patients coinfecting with TB and HIV were analysed by LC-MS/MS followed by non-linear mixed-effects modelling. Patients were genotyped for SLCO1B1 (463 C>A, 388 A>G, 11187 G>A, rs4149015, 521 T>C and 1436 G>C) and SLCO1B3 (334 T>G).

**Results:** One-compartment disposition models described the observations adequately. The oral clearances of rifampicin and 25-desacetyl-rifampicin were 140% and 110% higher, respectively, in patients on concomitant efavirenz-based ART. Rifampicin bioavailability was also lower in patients on concomitant ART. Further, although not included in the final model, a lower relative bioavailability in carriers of WT SLCO1B3 334 T>G compared with carriers of mutations in the genotype was estimated.

**Conclusions:** The results presented indicate both pre-systemic and systemic induction by efavirenz-based ART affecting rifampicin pharmacokinetics. The described drug–drug interaction has a clinical impact on rifampicin exposure prior to steady state and may impact the early bactericidal activity in patients on efavirenz-based ART.

### Introduction

Approximately one-third of all HIV-associated deaths are due to TB, making TB the most common cause of death in HIV-infected individuals.<sup>1</sup> Rifampicin is a key sterilizing drug in the currently used first-line TB therapy. A rifampicin peak plasma concentration ( $C_{max}$ ) of >8 mg/L has been suggested as a target therapeutic concentration.<sup>2</sup> The WHO recommends an adjusted daily dose of 10 mg/kg. However, due to the pharmacokinetic variability and exposure-dependent efficacy of rifampicin, doses up to 35 mg/kg are currently being investigated.<sup>3</sup> Rifampicin is primarily metabolized to the active metabolite 25-desacetyl-rifampicin by beta esterases.<sup>4</sup> Unknown elimination pathways of rifampicin are autoinduced and an up to 2-fold increase in oral clearance has been described at steady state compared with at initiation of anti-tubercular therapy.<sup>5</sup> Furthermore, rifampicin undergoes hepatic first-pass extraction and exhibits a non-linear relationship between dose and exposure.<sup>6,7</sup> In addition, polymorphism in SLCO1B1 genes coding for organic anion-transporting polypeptide 1B1 has been suggested to affect rifampicin exposure.<sup>8</sup>

Efavirenz-based ART is recommended as an alternative first-line treatment for HIV. Efavirenz is a known inducer of metabolic

enzymes.<sup>9</sup> Hence, there is a risk of drug–drug interactions affecting rifampicin pharmacokinetics during co-administration when concomitantly treating TB and HIV. Although an effect of HIV infection on rifampicin pharmacokinetics has been previously described,<sup>10</sup> HIV treatment has not shown any effect on pharmacokinetic parameters of rifampicin.<sup>11–13</sup> However, in those studies, HIV treatment was initiated at steady state of antitubercular therapy and genetic correlations were not evaluated. Thus, this study aimed to investigate the simultaneous effects of enzymatic polymorphisms and concomitant efavirenz-based ART on the pharmacokinetics of rifampicin and 25-desacetyl-rifampicin.

### Methods

#### Patients and study design

An open-label observational clinical study was performed in four clinics in Rwanda. Patients were either HIV-treatment naive (arm A) or treated for HIV (arm B) when TB therapy was initiated. Patients in each clinic were offered to participate in the study if inclusion criteria were met. Inclusion criteria were: 21–65 years of age, HIV-antibody positive, TB-drug naive and clinical diagnosis of TB. TB and HIV were managed according to domestic

guidelines.<sup>14</sup> Patients who were HIV-treatment naive were initiated on ART following 2–8 weeks of TB therapy depending on patient status.

Rifampicin-based fixed-dose combinations (FDCs) containing rifampicin, isoniazid, pyrazinamide and ethambutol at 150/75/400/275 mg (Svizera, Almere, The Netherlands) were administered to study participants. Weight-band-based doses were used as follows:  $\leq 28$  kg, one and a half tablets; 29–37 kg, two tablets; 38–54 kg, three tablets; 55–70 kg, four tablets; and  $\geq 71$  kg, five tablets (in order to administer a rifampicin dose of approximately 10 mg/kg). In addition to the FDCs, eight patients were administered streptomycin.

## Ethics

The clinical study was performed in agreement with the Helsinki Declaration and International Conference on Harmonization guidance for Good Clinical Practice. Approval to perform the study was received from the National Ethics Committee of the Ministry of Health in Rwanda (IRB 00001497). Patients provided a signed written informed consent and were informed that participation was voluntary and withdrawal was accepted at any time during the study.

## Dose intake and sample collection

Blood samples were collected prior to the first dose of rifampicin and at 1, 2, 3, 4, 6 and 8 h after the first dose. Plasma was harvested by centrifugation of the collected samples and then stored at  $-30^{\circ}\text{C}$  for 1 week in clinics before being transferred to  $-80^{\circ}\text{C}$  for long-term storage. Due to the observational nature of the study, no instructions regarding food intake in proximity to dose or during sample collection were specified in the study protocol. Blood samples to perform genotyping of SNPs were collected separately.

## Bioanalytics

Rifampicin and 25-desacetyl-rifampicin plasma concentrations were determined by LC-MS/MS.<sup>15</sup> The method was validated according to FDA guidelines<sup>16</sup> at a concentration range of 200–25 000 and 40–5000 ng/mL for rifampicin and 25-desacetyl-rifampicin, respectively. Intra-day accuracy and precision for rifampicin and 25-desacetyl-rifampicin were 92%–105% and  $<11\%$  relative standard deviation, respectively.

## Genotyping

A QIAamp DNA Blood Mini Kit was used to perform genomic DNA extraction from blood samples for genotyping of SLCO1B1 (463 C>A, 388 A>G, 11187 G>A, rs4149015, 521 T>C and 1436 G>C) and SLCO1B3 (334 T>G). Genotyping was performed by multiplexed primer extension chemistry of an iPLEX assay with detection of the incorporated allele by MS with a MassARRAY analyser (Agena Bioscience, San Diego, CA, USA).<sup>17,18</sup> The output data were converted into genotype data using Typer software (Agena Bioscience).

## Pharmacokinetic analysis

Modelling was carried out in NONMEM software, version 7.4.3 (ICON Development Solutions, Ellicott City, MD, USA).<sup>19</sup> Models were fitted to observations using first-order conditional estimation with interaction. Observations below the lower limit of quantification ( $n = 24$ ) were ignored. Perl-Speaks-NONMEM (version 4.8.1) and Pirana (version 2.9.8) were used for model automation and tracking of model development. R (version 3.5.1) with packages mrgsolve (version 0.10.1) and nonmem2R (version 0.2.1) was used for simulations with the final model and to create diagnostic plots, respectively.

A structural model for rifampicin was developed prior to adding 25-desacetyl-rifampicin observations. One- and two-compartment disposition models with first-order absorption and elimination were applied to

rifampicin observations. Discrimination between nested models was based on the objective function value (OFV). A difference in OFV is considered  $\chi^2$  distributed and a decrease in OFV ( $\Delta\text{OFV}$ ) of  $-3.84$  and  $-10.83$  is equivalent to a model improvement at a significance level of  $P < 0.05$  and  $P < 0.001$ , respectively. Different absorption models were applied in the model, including lag-time and transit-compartment models with either a fixed or estimated number of transit compartments.<sup>20</sup> Allometric scaling by body weight was applied to all clearance and volume parameters by a power of 0.75 and 1, respectively.<sup>21,22</sup>

One- and two-compartment disposition models were applied to 25-desacetyl-rifampicin observations. Rifampicin was assumed to be eliminated via two different metabolic pathways out of which one resulted in the formation of 25-desacetyl-rifampicin. A semi-mechanistic model including a liver compartment was evaluated to estimate the intrinsic clearance of rifampicin.<sup>12</sup> The hepatic volume, blood flow and fraction of unbound rifampicin plasma concentrations were then fixed to 2 L, 90 L/h and 0.2, respectively.<sup>23,24</sup> Inter-individual variability was evaluated on all estimated structural parameters as exponential random effects. Additive, proportional or combined residual errors were assessed separately for rifampicin and 25-desacetyl-rifampicin.

Covariates were tested by stepwise inclusion followed by stepwise elimination. Covariates were included and retained in the model at a significance level of 0.05 and 0.001, respectively. Continuous covariates tested were ALT, AST, age, serum creatinine, creatinine clearance as determined by the Cockcroft and Gault equation<sup>25</sup> and CD4 cell count. The continuous covariates were centred on their respective medians. Categorical covariates tested were sex, concomitant HIV therapy (study arm), study site and SLCO1B1 (463 C>A, 388 A>G, 11187 G>A, rs4149015, 521 T>C and 1436 G>C) and SLCO1B3 (334 T>G) genotypes. Individuals with missing genotypes ( $n = 7$ ) were categorized as a separate group in the initial screening of genotype covariates. Three approaches were evaluated for statistically significant covariates: including patients with missing genotypes as a separate category; assigning all patients with missing genotypes to the most common genotype; or using mixture models to assign patients with missing genotypes to different groups.<sup>26</sup> Differences in parameter estimates, OFV and plausibility of the estimated covariate effect were evaluated.

The final model was evaluated by parameter plausibility, goodness-of-fit plots and a prediction corrected visual predictive check (pcVPC) ( $n = 1000$ ). A bootstrap ( $n = 200$ ) was performed to calculate parameter precisions and CIs of the final model.

Stochastic simulations using the final model were performed to evaluate rifampicin exposure following a standard dose (10 mg/kg) and a high dose (35 mg/kg) depending on included covariates. Fixed parameters from a previously described model were used to account for the rifampicin non-linear increase in exposure with higher dose when evaluating high-dose rifampicin.<sup>5</sup> The non-linear increase in exposure with higher dose was applied on the bioavailability ( $F$ ) in the model according to the following equation:

$$F = 1 + \frac{0.504 \times (\text{dose} - 450)}{67 + (\text{dose} - 450)}$$

where 0.504 is the maximal increase in  $F$  and 67 (mg) is the increase in dose above 450 mg corresponding to 50% of the maximal increase in  $F$ .

## Results

### Pharmacokinetic analysis

In total, 874 concentration–time observations were included in the present analysis (raw data are shown in Figure 1). Out of the 63 patients included, 56 were genotyped. Patient characteristics are

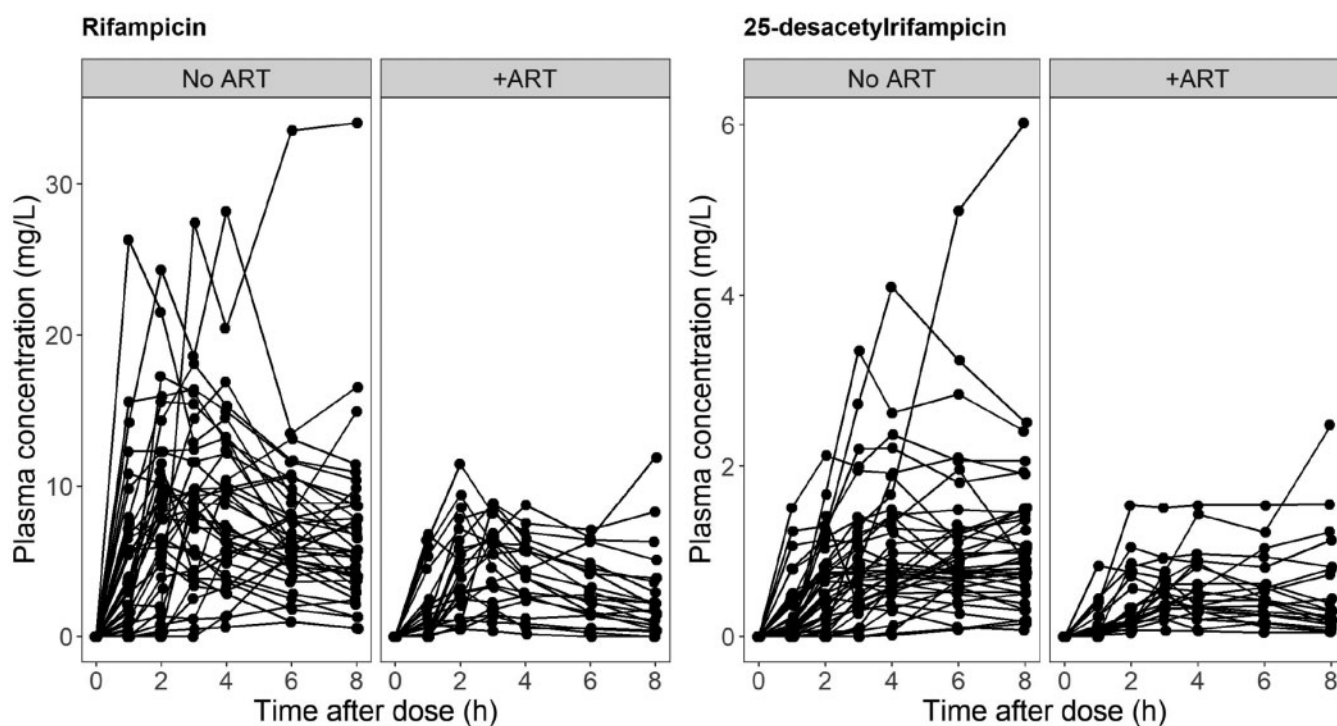


**Figure 1.** Plasma concentration–time profiles of rifampicin and its metabolite 25-desacetyl rifampicin in patients coinfected with HIV and TB following the first dose of rifampicin. Patients were either on concomitant efavirenz-based ART (+ART) or HIV-treatment naive (No ART).

**Table 1.** Demographics of adult Rwandan coinfected TB/HIV patients concurrently treated for both diseases or only treated for TB

	Concurrent HIV treatment <sup>a</sup>	HIV-treatment naive
Number of patients	23	40
Age (years)	40 (26–57)	38 (21–52)
Weight (kg)	48 (35–65)	50 (30–68)
Serum creatinine ( $\mu\text{mol/L}$ )	71 (44–159)	66 (35–159)
Creatinine clearance ( $\text{mL/min}$ )	81 (30–155)	84 (38–155)
AST ( $\text{U/mL}$ )	33 (11–248)	34 (11–131)
ALT ( $\text{U/mL}$ )	36 (9–126)	30 (5–101)
CD4 cell count ( $\text{cells/mm}^3$ )	230 (21–716)	240 (6–524)
Sex (female/male)	10/13	16/24
Rifampicin dose ( $\text{mg/day}$ )	300 ( $n=1$ ); 450 ( $n=13$ ); 600 ( $n=9$ )	300 ( $n=4$ ); 450 ( $n=22$ ); 600 ( $n=14$ )

Continuous data given as median (range).

Categorical data given as counts.

<sup>a</sup>HIV treatment includes efavirenz, lamivudine and zidovudine or tenofovir.

summarized in Table 1 and genotype frequencies are summarized in Table 2. The dispositions of rifampicin and 25-desacetyl rifampicin were most adequately described by one-compartment models. The absorption was described using a transit compartment model ( $n=1$ ) with an absorption rate constant equal to the transit rate. A pcVPC to illustrate the predictive properties of the model is shown in Figure 2. Whereas the observed median rifampicin

concentrations were in the upper range of its 95% CI, the model overall described the data adequately.

The oral clearance of rifampicin was 2.4-fold higher in patients on concomitant treatment with efavirenz-based ART ( $\Delta\text{OFV} = -12.9$ ) compared with patients who were ART naive. The  $\text{AUC}_{25\text{-desacetyl rifampicin}}/\text{AUC}_{\text{rifampicin}}$  ratio (non-compartmental analysis) was higher in patients on concomitant ART (0.14) compared with the patients who were ART naive (0.11) ( $P=0.008$ , Wilcoxon test). Adding an effect of ART on 25-desacetyl rifampicin clearance (2.1-fold increase) further reduced OFV by  $-13.0$ .

The relative bioavailability was significantly lower in patients on concomitant ART ( $\Delta\text{OFV} = -24.8$ ). Inter-individual variability in bioavailability was reduced from 114% to 82% when the effects of ART were added. Additionally, carriers of WT SLCO1B3 334 T>G had a lower relative bioavailability ( $-0.33$ ) compared with carriers of the heterozygous (T/G) or homozygous (G/G) mutation ( $\Delta\text{OFV} = -7.8$ ). A mixture model predicted all individuals with missing genotypes to be carriers of the SLCO1B3 334 T>G WT variant. Estimating separate effects for T/G carriers and G/G carriers did not result in a different OFV. Therefore, a combined effect for carriers of a mutation in the SNP was estimated. However, the effect of SLCO1B3 was excluded from the final model due to inadequate statistical significance. Parameter estimates and precisions of the final model are shown in Table 3.

### Simulations

The final model was used to simulate exposures ( $\text{AUC}_{0-24\text{h}}$  and  $C_{\text{max}}$ ) following the currently used dose (10 mg/kg) and high dose (35 mg/kg) of rifampicin. Simulations were stratified on whether

**Table 2.** Distribution of SLC01B1 and SLC01B3 SNPs in Rwandan patients coinfecting with TB and HIV ( $n = 56^a$ )

Genotype	Allele	Number (%)
SLC01B1		
463 C>A	C/C	53 (95)
	C/A	3 (5)
388 A>G	A/A	3 (5)
	A/G	15 (27)
	G/G	38 (68)
11187 G>A	G/G	48 (86)
	G/A	8 (14)
rs4149032	T/T	27 (48)
	T/C	21 (38)
	C/C	8 (14)
521 T>C	T/T	46 (82)
	T/C	10 (18)
1436 G>C	G/G	51 (91)
	G/C	5 (9)
SLC01B3		
334 T>G	T/T	24 (43)
	T/G	19 (34)
	G/G	13 (23)

<sup>a</sup>Number of individuals with missing genotypes = 7.

the patients were on concomitant ART or ART naive. The simulations predicted the majority of patients administered doses of 10 mg/kg in both groups to have a  $C_{max}$  below the value suggested to achieve an adequate therapeutic effect.<sup>2</sup> In patients on efavirenz-based ART, 35 mg/kg doses resulted in  $C_{max}$  values above the recommended threshold for a large proportion of the simulated patients. Figure 3 depicts simulated plasma concentration-time profiles following a 10 mg/kg or 35 mg/kg dose, depending on administration of efavirenz-based ART.

Simulations of exposure for a typical individual weighing 50 kg (the median weight in the dataset) predicted a mean  $AUC_{0-24h}$  of 76 mg·h/L in ART-naive patients and 19 mg·h/L in patients on ART for doses of 10 mg/kg (Table 4). For doses of 35 mg/kg, an  $AUC_{0-24h}$  of 455 mg·h/L and 106 mg·h/L was predicted in ART-naive patients and patients on ART, respectively.

## Discussion

A population pharmacokinetic model for rifampicin and 25-desacetyl-rifampicin was developed. The model was used to evaluate the effects of concomitant ART and genetic polymorphism on the pharmacokinetic parameters of rifampicin and its major metabolite. Rifampicin oral clearance was more than 2-fold higher in patients on concomitant ART compared with patients who were ART naive. Mechanistically, the findings could be explained by induction of hepatic metabolic enzymes by ART. Interestingly, the higher rifampicin clearance in patients on concomitant ART is close to the approximately 2-fold increase in rifampicin clearance after autoinduction observed in other studies.<sup>5,12</sup> Previous studies have suggested that rifampicin concentrations are similar between patients on concomitant efavirenz-based ART and patients who

are ART naive. If rifampicin and efavirenz-based ART induce the same pathway, the autoinduction could have masked such an interaction in previous studies since plasma concentrations have been measured at steady state of antitubercular therapy.<sup>11-13</sup>

Polymorphism in SLC01B1 has previously been suggested to affect rifampicin pharmacokinetics.<sup>8,27</sup> In the present cohort, an effect of SLC01B3 334 T>G on relative bioavailability was observed. The covariate was not included in the final model due to inadequate statistical significance and lack of prior knowledge on the effect of SLC01B3 polymorphism on rifampicin pharmacokinetics. However, if the effect is confirmed, the relatively large difference in exposure may make SLC0 a suitable factor for individualized therapy. Food intake affects rifampicin exposure and may partly have contributed to some of the variability in bioavailability.<sup>28,29</sup> However, since food intake was not documented in the clinical study, potential effects of food were not evaluated in the present analysis.

The lower bioavailability in patients on ART is similar to the decrease in rifampicin bioavailability (from 93% to 68%) during the first week of rifampicin administration reported by Loos *et al.*<sup>6</sup> The authors suggested a time-dependent increase in pre-hepatic metabolism of rifampicin, which was maximized after 1 week. In the present model, pre-hepatic and hepatic first-pass effects were estimated as total relative bioavailability, which may contribute to the estimated higher effect of ART on bioavailability compared with pre-hepatic autoinduction by rifampicin.<sup>6</sup> A semi-mechanistic model including a hepatic compartment to separate pre-hepatic bioavailability from the first-pass effect was evaluated. However, for such a model, 25-desacetyl-rifampicin would have to be assumed to be eliminated either via a hepatic route or via a non-hepatic route since two separate pathways would be unidentifiable. No such assumptions are required for an empirical model, which was therefore considered more suitable since esterases responsible for 25-desacetyl-rifampicin formation are present in both the liver and the blood.

Efavirenz induces CYP3A4 and P-glycoprotein, both of which may affect the bioavailability of drugs.<sup>30</sup> The turnover half-life of P-glycoprotein has been estimated to be 5–17 h, in contrast to the 70 h turnover half-life of CYP3A4.<sup>31,32</sup> The reduction in bioavailability maximized after 1 week in the study by Loos *et al.*<sup>6</sup> may plausibly be caused by induction of P-glycoprotein due to its shorter turnover half-life. Hence, the reduced bioavailability of rifampicin in our study could be explained by intestinal P-glycoprotein, which is fully induced following 1 week of efavirenz-based ART. P-glycoprotein may further be saturated at higher doses of rifampicin. Such a hypothesis is supported by higher serum rifampicin concentrations following inhibition of intestinal P-glycoprotein.<sup>33</sup>

Simulations predicted an average  $AUC_{0-24h}$  of 76 mg·h/L following the first dose of rifampicin in ART-naive patients. The prediction is well in line with a recent meta-analysis of rifampicin pharmacokinetics averaging a first-dose AUC of 72.6 mg·h/L.<sup>34</sup> Further, the simulations predicted an average  $AUC_{0-24h}$  of 19 mg·h/L in patients on concomitant ART. Such an exposure is at the lower end of the rifampicin steady-state AUCs presented by the meta-analysis and suggests a 75% reduction in rifampicin exposure in patients on efavirenz-based ART. In the simulations of 35 mg/kg doses a previously described non-linear increase in bioavailability with higher dose was included.<sup>5</sup> Despite inclusion of such non-linearity, the model predicted a 45% lower AUC in patients on ART

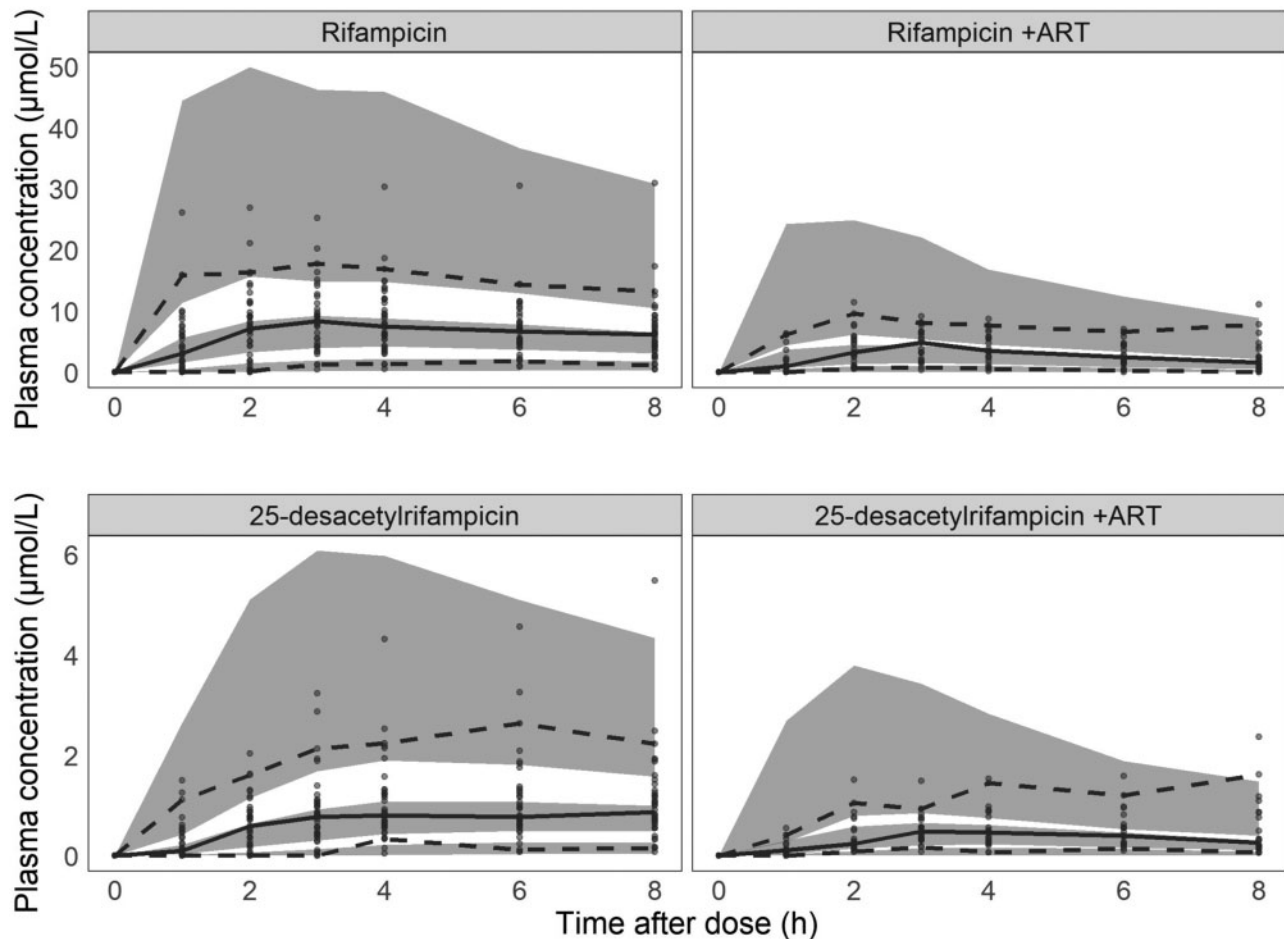


**Figure 2.** pcVPC ( $n = 1000$ ) for the final population pharmacokinetic model of rifampicin and 25-desacetylriofampicin stratified by concomitant ART. Circles are plasma concentration–time observations, the continuous line and the broken lines are the median and the 90th percentiles of the observed data, respectively, and the shaded areas represent the 95% CIs of the 5th, 50th and 95th percentiles predicted by the model.

**Table 3.** Parameter estimates of the final pharmacokinetic model of rifampicin in adult patients coinfecting with TB and HIV

Parameter	Population mean (%RSE)	95% CI	% IIV (%RSE)
$CL_{RIF}$ (L/h)	5.80 (12.9)	4.52 to 7.61	28.6 (34.5)
$F_m$	0.71 (16.5)	0.45 to 0.89	–
$V_{RIF}$ (L)	48.0 (11.0)	38.6 to 58.6	53.3 (41.0)
MTT (h)	1.65 (18.0)	1.2 to 2.5	139.5 (25.5)
$CL_{DERIF}$ (L/h)	29.6 (15.2)	21.2 to 37.8	–
Effect of ART on $CL_{RIF}$	+1.44 (39.6)	0.75 to 3.1	–
Effect of ART on $CL_{DERIF}$	+1.09 (44.3)	0.49 to 2.5	–
Relative $F$	1 fix	–	80.9 (23.1)
Effect of ART on $F$	–0.42 (42.7)	–0.003 to –0.61	–
Residual errors			
proportional, RIF (%)	41.7 (7.69)	34.5 to 46.3	–
proportional, DERIF (%)	36.5 (7.83)	31.0 to 41.9	–
additive, RIF ( $\mu\text{mol/L}$ )	0.001 fix	–	–
additive, DERIF ( $\mu\text{mol/L}$ )	0.001 fix	–	–

$CL_{RIF}$ , rifampicin oral clearance;  $F_m$ , fraction of rifampicin clearance forming 25-desacetylriofampicin;  $V_{RIF}$ , oral volume of distribution for rifampicin; MTT, mean transit time;  $CL_{DERIF}$ , clearance of 25-desacetylriofampicin;  $F$ , bioavailability; IIV, inter-individual variability; RSE, relative standard error.

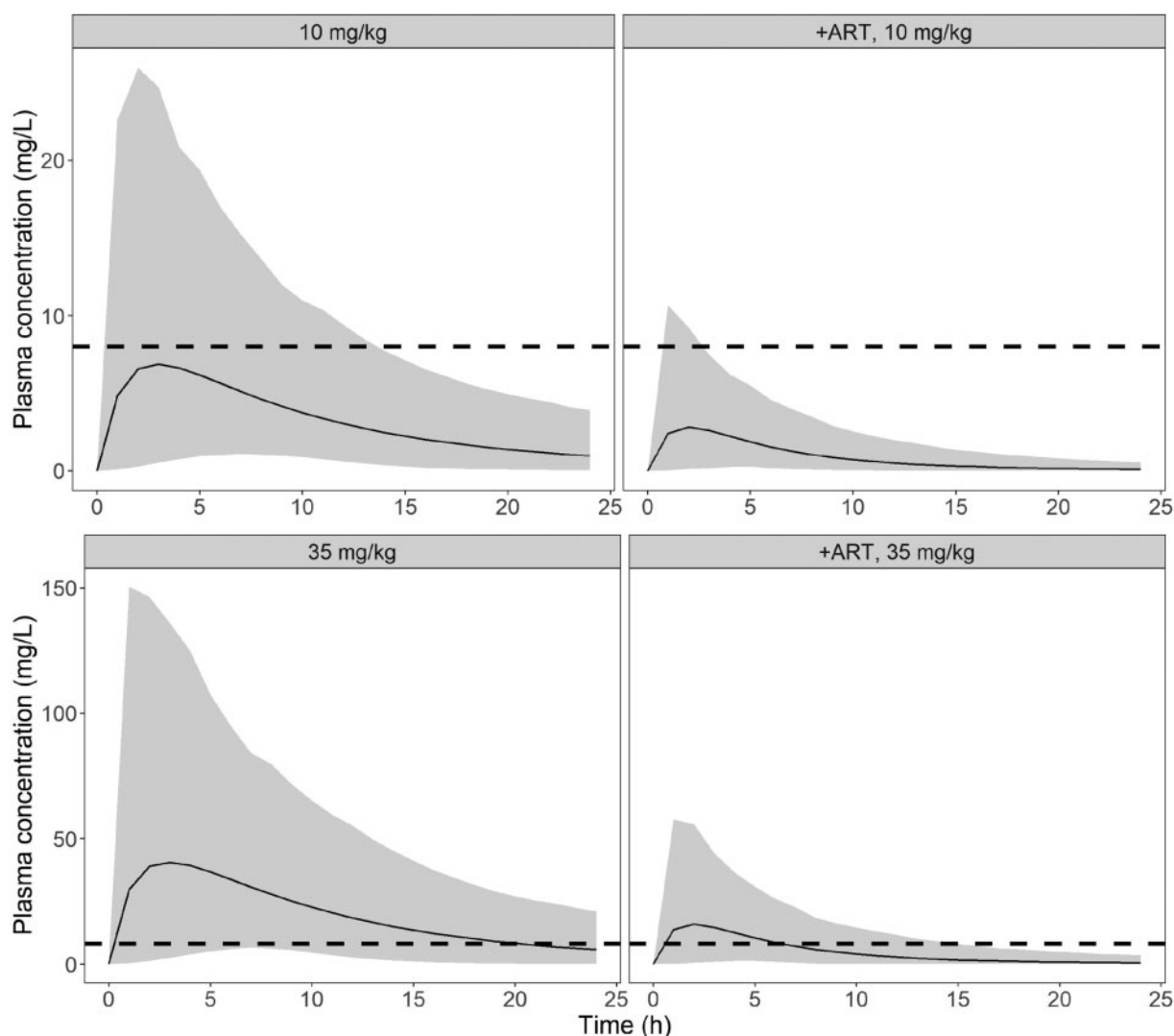


**Figure 3.** Simulated rifampicin plasma concentration–time profiles after the first dose (90% of the simulated data,  $n = 1000$ ) in patients on concomitant ART (+ART) or ART naive. The continuous line is the mean plasma concentration, the shaded area is the 95% range of the simulated data and the broken line is the therapeutic threshold (8 mg/L).

**Table 4.** Model predictions and clinically observed rifampicin  $AUC_{0-24h}$  (mg·h/L) at steady state after a standard dose and a high dose

	Rifampicin dose	
	10 mg/kg	35 mg/kg
Model prediction <sup>a</sup>		
first dose	76.1	455.0
ART induced	19.3	106.4
Meta-analysis <sup>34</sup>		
first dose	72.6	–
steady state	38.7	194.6

Data are given as geometric means.

<sup>a</sup>Prediction based on 1000 simulations of a typical individual weighing 50 kg.

compared with the average steady-state AUC observed in clinical trials. In addition to saturation in rifampicin clearance, the under-prediction of AUC may indicate saturation of the effect on pre-hepatic bioavailability. Thus, the effect of efavirenz-based ART may be proportionally smaller for higher doses of rifampicin. A study of the interaction at higher doses of rifampicin would give further answer to a potentially non-linear effect on pre-hepatic induction.

Simulations of 10 mg/kg doses indicated that the standard treatment results in too-low exposure of rifampicin. A dose of 35 mg/kg would result in a  $C_{max}$  above the recommended threshold for the majority of patients. Studies have shown that short-term (up to 12 weeks) treatment with 35 mg/kg rifampicin is safe<sup>3,35</sup> and ongoing clinical trials will further give answer to the tolerability of high-dose rifampicin. The results presented here indicate that the standard-dose regimen is inadequate in patients

coinfected with TB and HIV and that higher doses of rifampicin are crucial in the studied population.

A recent study showed no alteration of rifampicin pharmacokinetics by efavirenz-based ART at steady state.<sup>11</sup> Since no effect was observed at steady state, efavirenz-based ART plausibly affects rifampicin exposure equivalently to rifampicin autoinduction for both prehepatic and hepatic metabolism. The early bactericidal effect of rifampicin increases with dose and is exposure dependent.<sup>36</sup> Moreover, potentially shorter TB therapy with higher rifampicin doses has been proposed.<sup>37</sup> Whereas rifampicin bioavailability is autoinduced after the first week of TB therapy, autoinduction of rifampicin clearance is maximized after a few weeks. Patients on efavirenz-based ART will thus have a lower exposure to rifampicin for at least a few weeks compared with patients not yet initiated on ART. The initially lower rifampicin exposure in patients already on concomitant efavirenz-based ART at the initiation of TB therapy may have a significant impact on the early bactericidal effect of rifampicin. Therefore, potential differences in clinical outcome or time to sputum conversion due to the interaction described in the present study require evaluation.

In addition to an effect on rifampicin clearance, the clearance of 25-desacetyl-rifampicin was significantly higher in patients on concomitant ART. The effect on rifampicin clearance was higher than the effect on 25-desacetyl-rifampicin clearance. The results suggest that efavirenz-based ART induces both the formation and elimination of the metabolite resulting in a higher  $AUC_{25\text{-desacetyl-rifampicin},0-8h}/AUC_{rifampicin,0-8h}$  ratio in patients on ART. Rifampicin and efavirenz induce metabolic enzymes through activation of the nuclear pregnane X receptor and constitutive androstane receptor, respectively.<sup>38,39</sup> In addition, rifampicin has been shown to moderately induce beta esterases *in vitro*.<sup>40</sup> The results presented here indicate an induction of beta esterases by efavirenz. Although the efficacy contribution of 25-desacetyl-rifampicin is considered low, the protein binding of 25-desacetyl-rifampicin is not known, whereas the protein binding of rifampicin is approximately 80%.<sup>24</sup> If the protein binding of 25-desacetyl-rifampicin is lower, the efficacy contribution may be higher than previously suggested, assuming that only unbound drug or metabolite can have an effect. A 30% change in  $AUC_{25\text{-desacetyl-rifampicin}}/AUC_{rifampicin}$  is unlikely to be of clinical relevance, considering the low exposure to 25-desacetyl-rifampicin. However, the combined lower exposure to both rifampicin and 25-desacetyl-rifampicin may effect early bactericidal activity.

The present study had some limitations. Firstly, the model was developed on data from a standard-dose regimen and the changes in rifampicin pharmacokinetics following doses of 35 mg/kg are based on estimates from a previous model in TB patients. Secondly, the ART consisted of efavirenz, lamivudine and zidovudine/tenofovir and the drug responsible for the effect on rifampicin pharmacokinetics could not be identified. However, efavirenz is probably the cause of the drug–drug interaction due to its inductive properties. Thirdly, mechanistic conclusions regarding the change in metabolite/drug exposure ratio were not supported by the data. Nevertheless, induction of both 25-desacetyl-rifampicin formation and elimination is plausible.

In conclusion, a population pharmacokinetic model for rifampicin and its major metabolite 25-desacetyl-rifampicin in patients coinfecting with HIV and TB was developed. Concomitant treatment with efavirenz-based ART resulted in a significant decrease

in rifampicin and 25-desacetyl-rifampicin exposure. The described drug–drug interaction could potentially affect the time course of TB elimination due to a lower early bactericidal activity of rifampicin. Such an effect may increase the risk of resistance development.

## Acknowledgements

Genotyping of SLCO SNPs was performed using the SNP&SEQ Technology Platform in Uppsala ([www.genotyping.se](http://www.genotyping.se)). The facility is part of the National Genomics Infrastructure supported by the Swedish Research Council for Infrastructures and Science for Life Laboratory, Sweden. The SNP&SEQ Technology Platform is also supported by the Knut and Alice Wallenberg Foundation. We would like to thank Johanna Melin for fruitful discussions regarding model diagnostics and Paolo Denti for modelling-related input.

## Funding

The clinical study upon which this analysis is based was supported by the Swedish International Development Cooperation Agency (SIDA) as part of a bilateral Rwandan/Swedish collaboration on higher education. The present analysis was performed without further financial support.

## Transparency declarations

None to declare.

## Author contributions

J.S., A.Ä. and M.A. wrote the original manuscript. J.S., A.Ä. and M.A. designed the research. J.S. performed the research. J.S., A.Ä. and M.A. analysed the data. E.B. and M.A. wrote the clinical study protocol. E.B. was the clinical study coordinator.

## References

- 1 WHO. Factsheet on HIV-Associated TB. 2016. [https://www.who.int/tb/areas-of-work/tb-hiv/tbhiv\\_factsheet\\_2016.pdf](https://www.who.int/tb/areas-of-work/tb-hiv/tbhiv_factsheet_2016.pdf).
- 2 Peloquin CA. Using therapeutic drug monitoring to dose the antimycobacterial drugs. *Clin Chest Med* 1997; **18**: 79–87.
- 3 Boeree MJ, Diacon AH, Dawson R et al. A dose-ranging trial to optimize the dose of rifampin in the treatment of tuberculosis. *Am J Respir Crit Care Med* 2015; **191**: 1058–65.
- 4 Jamis-Dow CA, Katki AG, Collins JM et al. Rifampin and rifabutin and their metabolism by human liver esterases. *Xenobiotica* 1997; **27**: 1015–24.
- 5 Svensson RJ, Aarnoutse RE, Diacon AH et al. A population pharmacokinetic model incorporating saturable pharmacokinetics and autoinduction for high rifampicin doses. *Clin Pharmacol Ther* 2018; **103**: 674–83.
- 6 Loos U, Musch E, Jensen JC et al. Pharmacokinetics of oral and intravenous rifampicin during chronic administration. *Klin Wochenschr* 1985; **63**: 1205–11.
- 7 Ruslami R, Nijland HM, Alisjahbana B et al. Pharmacokinetics and tolerability of a higher rifampin dose versus the standard dose in pulmonary tuberculosis patients. *Antimicrob Agents Chemother* 2007; **51**: 2546–51.
- 8 Weiner M, Peloquin C, Burman W et al. Effects of tuberculosis, race, and human gene SLCO1B1 polymorphisms on rifampin concentrations. *Antimicrob Agents Chemother* 2010; **54**: 4192–200.
- 9 Habtewold A, Amogne W, Makonnen E et al. Pharmacogenetic and pharmacokinetic aspects of CYP3A induction by efavirenz in HIV patients. *Pharmacogenomics J* 2013; **13**: 484–9.

- 10** Daskapan A, Idrus LR, Postma MJ *et al.* A systematic review on the effect of HIV infection on the pharmacokinetics of first-line tuberculosis drugs. *Clin Pharmacokinet* 2019; **58**: 747–66.
- 11** Bhatt NB, Barau C, Amin A *et al.* Pharmacokinetics of rifampin and isoniazid in tuberculosis-HIV-coinfected patients receiving nevirapine- or efavirenz-based antiretroviral treatment. *Antimicrob Agents Chemother* 2014; **58**: 3182–90.
- 12** Chirehwa MT, Rustomjee R, Mthiyane T *et al.* Model-based evaluation of higher doses of rifampin using a semimechanistic model incorporating auto-induction and saturation of hepatic extraction. *Antimicrob Agents Chemother* 2016; **60**: 487–94.
- 13** McIlleron H, Rustomjee R, Vahedi M *et al.* Reduced antituberculosis drug concentrations in HIV-infected patients who are men or have low weight: implications for international dosing guidelines. *Antimicrob Agents Chemother* 2012; **56**: 3232–8.
- 14** WHO. WHO Guidelines Approved by the Guidelines Review Committee. Consolidated Guidelines on the Use of Antiretroviral Drugs for Treating and Preventing HIV Infection: Recommendations for a Public Health Approach. 2013.
- 15** Sundell J, Bienvenu E, Birgersson S *et al.* Simultaneous quantification of four first line antitubercular drugs and metabolites in human plasma by hydrophilic interaction chromatography and tandem mass spectrometry. *J Chromatogr B Analyt Technol Biomed Life Sci* 2019; **1105**: 129–35.
- 16** US Department of Health and Human Services, FDA. Guidance for Industry Bioanalytical Method Validation. 2018. <https://www.fda.gov/regulatory-information/search-fda-guidance-documents/bioanalytical-method-validation-guidance-industry>.
- 17** Pusch W, Wurmbach JH, Thiele H *et al.* MALDI-TOF mass spectrometry-based SNP genotyping. *Pharmacogenomics* 2002; **3**: 537–48.
- 18** Gabriel S, Ziaugra L, Tabbaa D. SNP genotyping using the Sequenom MassARRAY iPLEX platform. *Curr Protoc Hum Genet* 2009; **Chapter 2**: Unit 2.12.
- 19** Beal S, Boeckmann A, Sheiner L. (1989-2009) *NONMEM Users Guides*. Icon Development Solutions.
- 20** Savic RM, Jonker DM, Kerbusch T *et al.* Implementation of a transit compartment model for describing drug absorption in pharmacokinetic studies. *J Pharmacokinet Pharmacodyn* 2007; **34**: 711–26.
- 21** Anderson BJ, Holford NH. Mechanistic basis of using body size and maturation to predict clearance in humans. *Drug Metab Pharmacokinet* 2009; **24**: 25–36.
- 22** McLeay SC, Morrish GA, Kirkpatrick CM *et al.* The relationship between drug clearance and body size: systematic review and meta-analysis of the literature published from 2000 to 2007. *Clin Pharmacokinet* 2012; **51**: 319–30.
- 23** Shepard TA, Lockwood GF, Aarons LJ *et al.* Mean residence time for drugs subject to enterohepatic cycling. *J Pharmacokinet Biopharm* 1989; **17**: 327–45.
- 24** Verbeeck RK, Singu BS, Kibuule D. Clinical significance of the plasma protein binding of rifampicin in the treatment of tuberculosis patients. *Clin Pharmacokinet* 2019; **58**: 1511–5.
- 25** Cockcroft DW, Gault MH. Prediction of creatinine clearance from serum creatinine. *Nephron* 1976; **16**: 31–41.
- 26** Keizer RJ, Zandvliet AS, Beijnen JH *et al.* Performance of methods for handling missing categorical covariate data in population pharmacokinetic analyses. *AAPS J* 2012; **14**: 601–11.
- 27** Chigutsa E, Visser ME, Swart EC *et al.* The SLCO1B1 rs4149032 polymorphism is highly prevalent in South Africans and is associated with reduced rifampin concentrations: dosing implications. *Antimicrob Agents Chemother* 2011; **55**: 4122–7.
- 28** Lin HC, Yu MC, Liu HJ *et al.* Impact of food intake on the pharmacokinetics of first-line antituberculosis drugs in Taiwanese tuberculosis patients. *J Formos Med Assoc* 2014; **113**: 291–7.
- 29** Peloquin CA, Namdar R, Singleton MD *et al.* Pharmacokinetics of rifampin under fasting conditions, with food, and with antacids. *Chest* 1999; **115**: 12–8.
- 30** Sankatsing SU, Beijnen JH, Schinkel AH *et al.* P-glycoprotein in human immunodeficiency virus type 1 infection and therapy. *Antimicrob Agents Chemother* 2004; **48**: 1073–81.
- 31** Lee SD, Osei-Twum JA, Wasan KM. Dose-dependent targeted suppression of P-glycoprotein expression and function in Caco-2 cells. *Mol Pharm* 2013; **10**: 2323–30.
- 32** Magnusson MO, Dahl ML, Cederberg J *et al.* Pharmacodynamics of carbamazepine-mediated induction of CYP3A4, CYP1A2, and Pgp as assessed by probe substrates midazolam, caffeine, and digoxin. *Clin Pharmacol Ther* 2008; **84**: 52–62.
- 33** Prakash J, Velpandian T, Pande JN *et al.* Serum rifampicin levels in patients with tuberculosis: effect of P-glycoprotein and CYP3A4 blockers on its absorption. *Clin Drug Investig* 2003; **23**: 463–72.
- 34** Stott KE, Pertinez H, Sturkenboom MGG *et al.* Pharmacokinetics of rifampicin in adult TB patients and healthy volunteers: a systematic review and meta-analysis. *J Antimicrob Chemother* 2018; **73**: 2305–13.
- 35** Boeree MJ, Heinrich N, Aarnoutse R *et al.* High-dose rifampicin, moxifloxacin, and SQ109 for treating tuberculosis: a multi-arm, multi-stage randomised controlled trial. *Lancet Infect Dis* 2017; **17**: 39–49.
- 36** Svensson RJ, Svensson EM, Aarnoutse RE *et al.* Greater early bactericidal activity at higher rifampicin doses revealed by modeling and clinical trial simulations. *J Infect Dis* 2018; **218**: 991–9.
- 37** Svensson EM, Svensson RJ, Te Brake LHM *et al.* The potential for treatment shortening with higher rifampicin doses: relating drug exposure to treatment response in patients with pulmonary tuberculosis. *Clin Infect Dis* 2018; **67**: 34–41.
- 38** Michaud V, Ogburn E, Thong N *et al.* Induction of CYP2C19 and CYP3A activity following repeated administration of efavirenz in healthy volunteers. *Clin Pharmacol Ther* 2012; **91**: 475–82.
- 39** Chen J, Raymond K. Roles of rifampicin in drug–drug interactions: underlying molecular mechanisms involving the nuclear pregnane X receptor. *Ann Clin Microbiol Antimicrob* 2006; **5**: 3.
- 40** Staudinger JL, Xu C, Cui YJ *et al.* Nuclear receptor-mediated regulation of carboxylesterase expression and activity. *Expert Opin Drug Metab Toxicol* 2010; **6**: 261–71.